BIOCHEMISTRY
including biophysical chemistry & molecular biology

Article

pubs.acs.org/biochemistry

# Single-Molecule Analysis of Thymine Dimer-Containing G-Quadruplexes Formed from the Human Telomere Sequence

Anna H. Wolna, Aaron M. Fleming, and Cynthia J. Burrows*

Department of Chemistry, University of Utah, 315 South 1400 East, Salt Lake City, Utah 84112-0850, United States

Supporting Information

**ABSTRACT:** The human telomere plays crucial roles in maintaining genome stability. In the presence of suitable cations, the repetitive 5′-TTAGGG-3′ human telomere sequence can fold into G-quadruplexes that adopt the hybrid, basket, or propeller fold. The telomere sequence is hypersensitive to UV-induced thymine dimer (T=T) formation, yet it does not cause telomere shortening. In this work, the potential structural disruption and thermodynamic stability of the T=T-containing natural telomere sequences were studied to understand why this damage is tolerated in telomeres. First, established methods, such as thermal melting measurements, electrophoretic mobility shift assays, and circular dichroism spectroscopy, were utilized to determine the effects of the damage on these structures. Second, a single-molecule ion channel recording technique using $\alpha$-hemolysin ($\alpha$-HL) was employed to examine further the structural differences between the damaged sequences. It was observed that the damage caused slightly lower thermal stabilities and subtle changes in the circular dichroism spectra for hybrid and basket folds. The $\alpha$-HL experiments determined that T=Ts disrupt double-chain reversal loop formation but are tolerated in edgewise and diagonal loops. The largest change was observed for the T=T-containing natural telomere sequence when the propeller fold (all double-chain reversal loops) was studied. On the basis of the $\alpha$-HL experiments, it was determined that a triplexlike structure exists under conditions that favor a propeller structure. The biological significance of these observations is discussed.

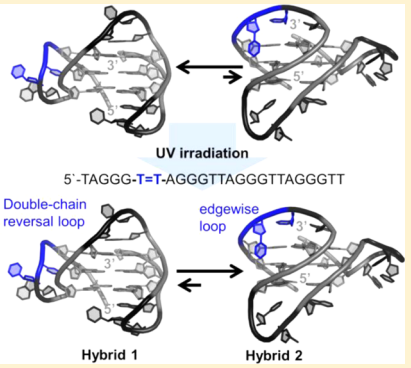


Telomeres are DNA−protein complexes that are essential to maintaining genome integrity.[1] Human telomere DNA consists of a 5′-$(TTAGGG)_n$-3′ repetitive sequence that is 5000−20000 bp long with a 3′ single-stranded overhang of 100−250 bases.[2,3] This guanine (G)-rich single-stranded DNA (ssDNA) sequence can form G-quadruplex structures that were recently validated in human cells.[4] The building unit of a G-quadruplex is a G-quartet that consists of four planar Gs that are hydrogen-bonded through the Hoogsteen face.[5] These alternative DNA secondary structures are proposed to play an important role in DNA recombination, transcription, and replication.[6−9] The ends of chromosomes are capped by telomeres to prevent fusion of the uncapped end of a chromosome with another telomere or a double-strand break and to prevent nucleolytic resectioning.[10,11] Understanding the secondary structure of G-quadruplexes is a key step to addressing their role in biological processes.

G-Quadruplexes can assume several different structures that are dependent upon the alkali metal ion ($K^+$ or $Na^+$) coordinated, the physical conditions of the solution, and the sequence. In a KCl solution, the human telomere sequence (hTelo) adopts two interchangeable structures termed hybrid 1 and hybrid 2 that display two edgewise loops and one double-chain reversal loop.[12−14] The main difference between these hybrid folds is the order of the loops, in which hybrid 1 has the double-chain reversal loop closest to the 5′ end and hybrid 2 has it closest to the 3′ end (Figure 1a). The basket fold occurs in a NaCl solution, and it contains two edgewise loops and one central diagonal loop (Figure 1a).[15] A third topology has been characterized and termed the propeller fold; it has been observed in highly dehydrating solutions or in solid-state experiments.[16−18] The propeller fold is formed in the presence of $K^+$ and contains only double-chain reversal loops (Figure 1a);[16,17,19] it is also commonly observed in various promoter sequences that are capable of G-quadruplex formation.[20] On the basis of the higher concentration of $K^+$ inside the cell,[21] and the higher G-quadruplex binding constant for binding to $K^+$ versus $Na^+$, the hybrid folds are the G-quadruplex conformations that were proposed to exist *in vivo* for hTelo,[13,22,23] and the folding pattern that it assumes is crucial for its proper function in the cell.[24,25]

The telomere sequence is hypersensitive to oxidative and UV-induced DNA damage that can alter its folding pattern.[27−29] Oxidative stress is a known contributor to telomere shortening that is directly associated with cell mortality and aging.[30−32] Guanine (G) is the most oxidation-prone DNA base because of its low redox potential;[33,34] consequently, the G-rich telomere sequence is hypersensitive to oxidative DNA damage,[28,35] and indeed, the majority of the G oxidation products were found to be present in the human telomere sequence.[35] Surprisingly, even though the damage

**Received:** August 25, 2014
**Revised:** November 14, 2014
**Published:** November 19, 2014

   dx.doi.org/10.1021/bi501072m | *Biochemistry* 2014, 53, 7484−7493

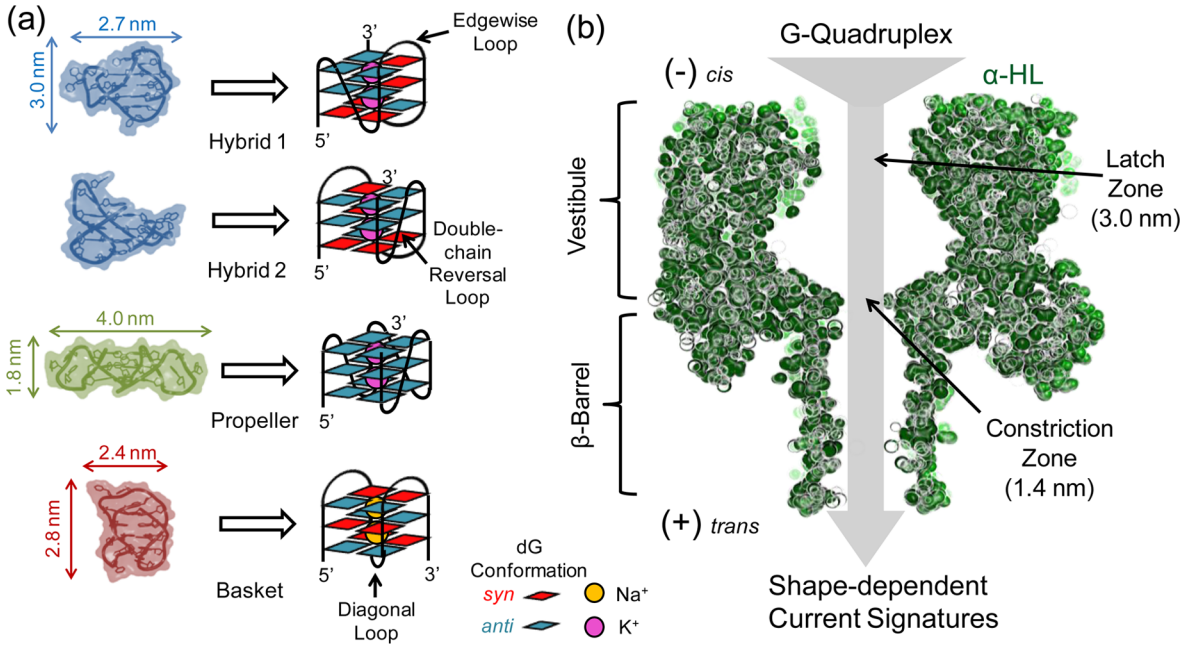


**Figure 1.** Nanopore measurements of G-quadruplexes in the $\alpha$-hemolysin ($\alpha$-HL) nanopore. (a) Space filling and schematic structures for the G-quadruplex folds: propeller [Protein Data Bank (PDB) entry 1KF1],[16] basket (PDB entry 143D),[15] hybrid type 1 (PDB entry 2JSK),[12] and hybrid type 2 (PDB entry 2JSQ).[12] (b) Experimental setup. $\alpha$-HL (PDB entry 7AHL)[26] was first assembled into a lipid bilayer, and then a voltage was applied across the channel. Current levels were measured when G-quadruplexes were captured in the vestibule.

disturbs the core of the G-quadruplex structure (G-tetrads), it still can maintain some degree of secondary structure, depending on the location of the damage.[35−37] In contrast to the core damage, DNA lesions found in the loops of G-quadruplex folds are well tolerated. Thymine glycol and 8-oxo-7,8-dihydro-2′-deoxyadenosine (8-oxo-A) present in the loops of hybrid and basket G-quadruplexes did not prevent folding, yielding similar structures.[36,38] Interestingly, the stabilities of these structures were dependent on the nature of the damage.[36,38]

Another type of persistent DNA damage is UV-induced photo-cross-linking of two adjacent thymine (T) residues resulting in the formation of *cis,syn*-thymine dimers [T=T (Scheme 1)].[39] The native human telomere sequence is

**Scheme 1. Two Adjacent Ts Are Converted to a *cis,syn*-Thymine Dimer (T=T) upon UV Irradiation**

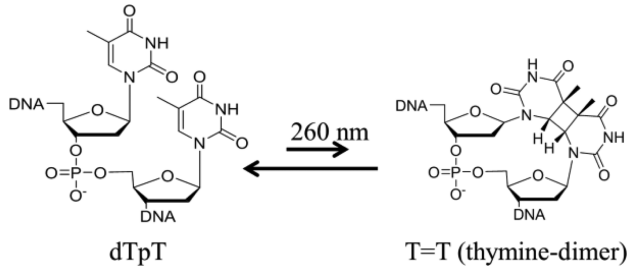


perfectly poised for T=T formation. This damage is readily formed in the epidermis and correlates with skin cancer;[40] in addition, model studies of UV damage to cells identified the telomere to be hypersensitive to formation of T=Ts.[27] Moreover, T=Ts in the telomeres were shown not to increase the level of shortening, and these cells did not show increased rates of apoptosis.[27] These results suggest that T=Ts are not detrimental to telomere structure and function. Despite the fact that the telomere region is hypersensitive to UV light-induced DNA damage,[27] few studies have been conducted on the effects of T=T in G-quadruplexes. An *in vitro* study conducted by Taylor's laboratory showed the hybrid folds can be UV-irradiated to form T=Ts.[41,42]

In this work, we investigated the stability and structure of T=T-containing G-quadruplexes to address the question how UV-induced damage affects human telomere G-quadruplex structure. These studies included established methods of analysis (circular dichroism, electrophoretic mobility shift assay, and thermal melting), as well as a new single-molecule method developed in our laboratory.[43,44] In this method, a single $\alpha$-hemolysin ($\alpha$-HL) nanopore was used to capture the different G-quadruplexes in the vestibule under an electrophoretic force. During the capture event, the recorded ion current gives characteristic patterns based on the G-quadruplex fold that was captured in the vestibule (Figure 1b).

## MATERIALS AND METHODS

**DNA Preparation and Purification.** The oligodeoxynucleotides (ODNs) were synthesized at the DNA/Peptide Core Facility at the University of Utah using commercially available phosphoramidites (Glen Research). The ODNs were then deprotected[45] and purified via high-performance liquid chromatography (HPLC) following standard protocols that are further explained in the Supporting Information (Experimental and Figure S1) .

**Circular Dichroism (CD) and $T_m$ Study.** To induce the hybrid folds, a 950 mM LiCl, 50 mM KCl, 25 mM Tris, 1 mM EDTA, pH 7.9 solution was used; the basket folds were induced with a 1 M NaCl, 25 mM Tris, 1 mM EDTA, pH 7.9 solution, and the propeller fold was induced with a 5 M LiCl, 20 mM KCl, 25 mM Tris, 1 mM EDTA, pH 7.9 solution. The ODNs were annealed by first heating the samples to 90 °C and then cooling them to room temperature over 4 h; next, the samples


dx.doi.org/10.1021/bi501072m | *Biochemistry* 2014, 53, 7484−7493

were stored at 4 °C for 2 days. The thermal denaturation studies were conducted by measuring the absorbance at a wavelength of 295 nm for basket and hybrid folds and at 260 nm for the propeller folds. The CD profiles were recorded on 20 $\mu$M samples at 20 °C in each of the salts described above. Plots of molar ellipticity were achieved using an $\varepsilon_{260}$ of 0.2805 L $\mu M^{-1}$ $cm^{-1}$ for the native sequence and an $\varepsilon_{260}$ of 0.2637 L $\mu M^{-1}$ $cm^{-1}$ for the T=T-containing sequences. The different values reflect the fact that T=T does not absorb light at 260 nm.

**Current Time Recordings.** The ion channel recordings were conducted with a custom-built amplifier and data acquisition system designed by Electronic BioSciences (EBS, San Diego, CA). The glass nanopore membrane (GNM) was fabricated using previously established procedures.[46,47] The data were collected at 21 ± 1 °C using a 500 kHz sampling rate and 100 kHz low-pass filter; however, for the purpose of presentation, the data were refiltered to 20 kHz. The data were then analyzed using QUB 1.5.0.31 and fit using OriginPro 9.1. For each ODN, three voltages were studied, 120, 140, and 160 mV (*trans* vs *cis*). For each voltage, roughly 1000 events were collected.

## RESULTS

**Characterization of Thymine Dimer-Containing G-Quadruplexes Using Conventional Methods.** The T=T-containing human telomere sequences chosen for the study were synthesized from commercially available phosphoramidites. The T=T was introduced at one of three places along the truncated native sequence of the human telomere sequence that could fold into a single G-quadruplex possessing a tail at both ends comprised of two nucleotides (Table 1). CD spectroscopy, thermal denaturation studies ($T_m$), and electrophoretic mobility shift assays (EMSAs) were conducted on each sequence under the following high-ionic strength conditions, which are required to conduct the ion channel recordings in the $\alpha$-HL nanopore:[43,44] (1) 50 mM KCl and 950 mM LiCl (hybrid folds), (2) 1 M NaCl (basket folds), or (3) 20 mM KCl with 5 M LiCl (propeller folds). All samples were in 25 mM Tris (pH 7.9) with 1 mM EDTA. The 5 M LiCl solution was previously shown by our laboratory to induce the propeller fold because of its dehydrating effect.[44] These data were compared to those collected under low-ionic strength conditions in the following salts: (1) 140 mM KCl and (2) 140 mM NaCl in phosphate buffer (pH 7.4).

**Table 1. T=T-Containing Human Telomere G-Quadruplex Sequences Studied**

| name | sequence |
|---|---|
| native sequence | 5′-TAGGGTTAGGGTTAGGGTTAGGGTT-3′ |
| 5′ T=T | 5′-TAGGG**T=T**AGGGTTAGGGTTAGGGTT-3′ |
| M T=T | 5′-TAGGGTTAGGG**T=T**AGGGTTAGGGTT-3′ |
| 3′ T=T | 5′-TAGGGTTAGGGTTAGGG**T=T**AGGGTT-3′ |

First, CD measurements were conducted for the natural sequence under the three different high-ionic strength salt conditions. The natural telomere sequence gave data that were consistent with literature reports (Figure 2).[48] Next, the T=T-containing G-quadruplexes were tested and found to give characteristic antiparallel (hybrid and basket) signatures with positive peaks at ∼290 nm (Figure 2a,b). Additionally, the hybrid folds featured a characteristic shoulder at 265 nm and a negative peak at 240 nm (Figure 2a). The basket fold featured

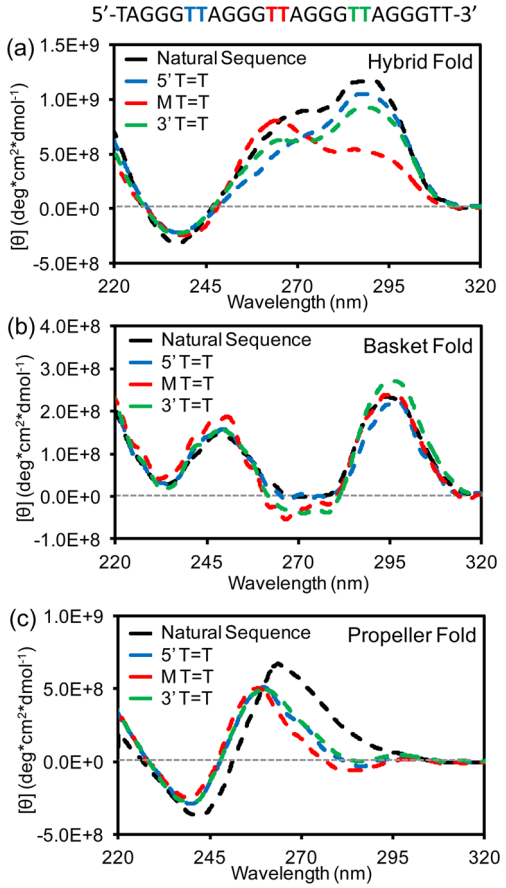


**Figure 2.** CD spectra of the human telomeric G-quadruplexes. The sequences are color coded as follows: blue for T=T in the 5′ loop, red for T=T in the middle loop (M T=T), green for T=T in the 3′ loop of the quadruplex, and black for the native sequence. (a) Hybrid fold: annealed in a 950 mM LiCl, 50 mM KCl, 25 mM Tris, 1 mM EDTA, pH 7.9 solution. (b) Basket fold: annealed in a 1 M NaCl, 25 mM Tris, 1 mM EDTA, pH 7.9 solution. (c) Propeller fold: annealed in a 5 M LiCl, 20 mM KCl, 25 mM Tris, 1 mM EDTA, pH 7.9 solution.

an additional positive peak at ∼240 nm and a trough at ∼265 nm (Figure 2b). These data led to the conclusion that the T=T-containing ODNs fold to the hybrid and basket topologies in the presence of $K^+$ and $Na^+$, respectively. As verification that the high-ionic strength conditions do not change the folding patterns, these data were compared to CD data that were obtained at a relevant ionic strength of 140 mM. The data look the same between the two different salt concentrations (Figure S7 of the Supporting Information). This is interpreted to mean that the high ionic strength does not change the overall structure of the quadruplexes. In contrast to the antiparallel folds, the propeller fold (parallel stranded) featured an intense peak at ∼264 nm and a negative peak at 240 nm. The T=T-containing ODNs were shifted by ∼5 nm toward shorter wavelengths compared to the natural sequence (Figure 2c). These data suggest that the T=T-containing human telomere sequence adopted a fold slightly different from the propeller fold in high molar concentrations of LiCl (5 M). The recorded CD spectra for these lesion-bearing G-quadruplexes were similar to the CD spectrum reported for the triplex folding sequence 5′-TTA$(GGGTTA)_3$-3′.[18,49,50] However, these data did not allow us to further confirm this observation.

Next, we examined the thermal stability of T=T-containing ODNs by monitoring the UV−vis absorption spectral change


dx.doi.org/10.1021/bi501072m | *Biochemistry* 2014, 53, 7484−7493

as a function of increased temperature. The $T_m$ of each fold is reported in Table 2, and representative $T_m$ curves are included in Figure S2 of the Supporting Information. In a KCl solution that induces the hybrid fold, the T=T-containing ODNs showed $T_m$ values ($\Delta T_m \sim -4$ °C) slightly lower than that of the native sequence, indicating that the presence of T=T only slightly destabilized the structure. Similarly, in a NaCl solution that gives the basket fold, the T=T-containing strands had $T_m$ values ($\Delta T_m \sim -4$ °C) slightly lower than that of the native sequence, again indicating the slightly lower stability of the damage-containing G-quadruplexes. In the solution that induces the propeller fold, the $T_m$ values were dependent on the location of the T=T. The largest decrease in $T_m$ ($\Delta T_m \sim -10$ °C) was observed when the T=T was positioned in the middle loop of a propeller fold; when the T=T was positioned in either the 5′ or 3′ loop, the $T_m$ was slightly lower than that of the native sequence ($\Delta T_m \sim -5$ °C).

**Table 2. $T_m$ Values for the G-Quadruplex Folds Studied**

| | $T_m$ (°C) | | |
|---|---|---|---|
| | hybrid fold[a] | basket fold[b] | propeller fold[c] |
| natural sequence | 59.9 ± 0.8 | 74.5 ± 0.3 | 54.2 ± 0.9 |
| 5′ T=T | 54.4 ± 0.5 | 69.2 ± 0.8 | 51.0 ± 0.6 |
| 3′ T=T | 57.3 ± 0.4 | 68.8 ± 0.5 | 49.4 ± 0.4 |
| M T=T | 55.8 ± 0.5 | 71.5 ± 0.6 | 43.9 ± 0.7 |

[a]In a 50 mM KCl, 950 mM LiCl, 25 mM Tris, 1 mM EDTA, pH 7.9 solution. [b]In a 1 M NaCl, 25 mM Tris, 1 mM EDTA, pH 7.9 solution. [c]In a 5 M LiCl, 20 mM KCl, 25 mM Tris, 1 mM EDTA, pH 7.9 solution.

Finally, we conducted EMSA experiments in NaCl or KCl to further support the ability of T=T-containing telomere sequences to fold into G-quadruplex structures (Figure S2 of the Supporting Information). All T=T-containing strands migrated approximately the same distance as the natural sequence. This experiment could not be performed for the propeller fold because of the 5 M LiCl that was required to induce this topology. The methods mentioned so far indicate that the T=T-containing human telomere sequences folded into G-quadruplexes are slightly less stable than the undamaged ODNs in the presence of $K^+$ and $Na^+$. The CD spectra for the damaged G-quadruplexes in KCl and NaCl lead to minor changes, suggesting that incorporation of T=T into the loops does not dramatically alter the quadruplex folds. Lastly, in 5 M LiCl, the human telomere sequence assumes a propeller fold; however, the damage-containing ODNs presented subtle perturbations to the CD spectra that are challenging to interpret by these methods. To gain more insight into the structural differences between the damage-containing folds, a single-molecule experiment was conducted with the $\alpha$-HL ion channel. This method has been recently developed in our laboratory to discriminate different topologies of G-quadruplexes.[43,44] Furthermore, the technique provides population information about an equilibrating mixture of species in solution.

**Single-Molecule Analysis of the Thymine Dimer-Containing G-Quadruplexes.** The nanopore recordings were conducted according to previously established procedures from the White laboratory.[46,47] Briefly, the wild-type $\alpha$-HL nanopore was assembled from monomers into a lipid bilayer that was painted across a glass nanopore membrane. A voltage was applied across the membrane, and the DNA was electrophoretically driven toward the *cis* side of the $\alpha$-HL (Figure 1b). Different G-quadruplex folds can yield unique current signatures by interacting differently with the $\alpha$-HL nanocavity.[43,44] We took advantage of this system to understand the folding patterns of T=T-containing G-quadruplexes in the three different salt solutions.

The T=T's effect on the G-quadruplex folds was interpreted by comparison to our recent results.[43] Previously, when the G-quadruplexes in a KCl solution interact with the vestibule of $\alpha$-HL, three unique ion−current patterns were observed. The ion−current patterns corresponding to the hybrid 1 and 2 folds were determined by reinforcing a single hybrid fold with 8-bromo-2′-deoxyguanosine, which forces G to adopt the *syn* conformation. In these studies, event types that corresponded to the hybrid 1 and hybrid 2 folds were uniquely identified. The third ion−current pattern was determined to be a triplexlike fold based on comparison to current patterns from a control strand that has three G runs and yields only a triplexlike fold. From these results, it was determined that the native telomere

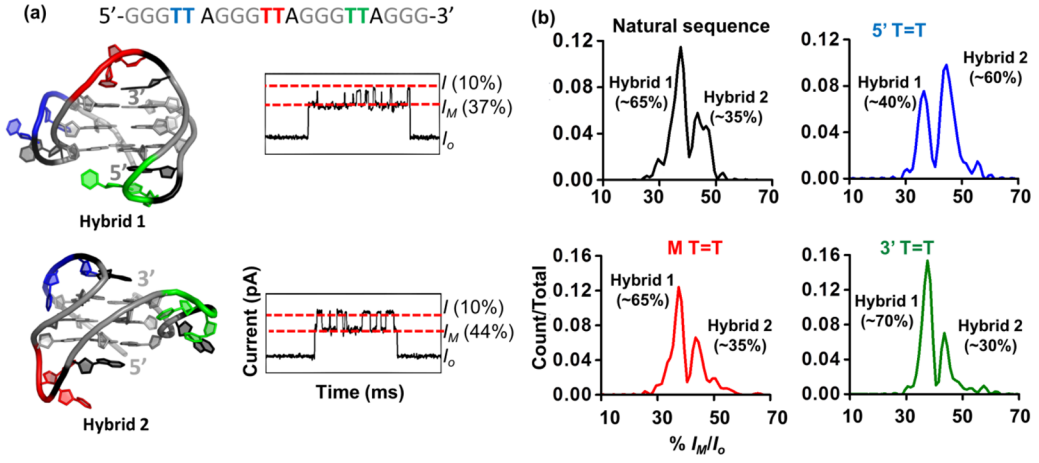


**Figure 3.** Analysis of hybrid 1 and hybrid 2 folds for G-quadruplexes containing the damaged base in different positions along the human telomere sequence at a single-molecule level. (a) Human telomere sequence with the positions of the T=T colored blue, red, and green followed by the structure of hybrid type 1 (PDB entry 2JSK)[12] and type 2 (PDB entry 2JSQ)[12] with their representative current−time ($i$−$t$) trace signatures. (b) Current histograms representing % $I_M/I_0$ of the events characteristic of the hybrid folds.


dx.doi.org/10.1021/bi501072m | *Biochemistry* 2014, 53, 7484−7493

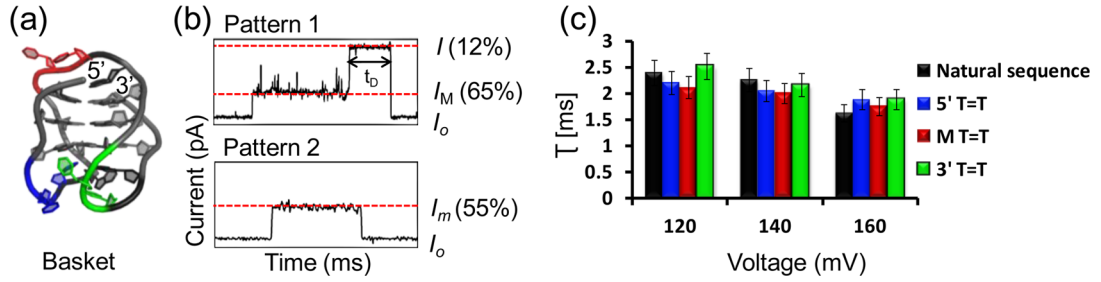


**Figure 4.** Nanopore analysis of the basket fold. (a) Structure of a basket (PDB entry 143D)[15] with the different positions of the T=T color-coded. (b) Representative *i*−*t* traces for the two different types of events observed. (c) Voltage dependence studies in which the translocation times ($t_D$) of ∼500 events were fit to an exponential decay model.

sequence exists in a hybrid 1:hybrid 2:triplexlike ratio of 11:5:1 ratio. These previous studies allowed us to compare ion−current patterns when T=T was placed in a loop to those from the native structures.

**Hybrid Folds.** First, the native sequence was studied under conditions that yield the hybrid folded G-quadruplex. In the presence of $K^+$, entry of the G-quadruplex folds produced three different event types. They represent the hybrid folds, loop entry (shallow blockage only, no translocation) and triplexlike folds, similar to the results of our previous report (Figure S3 of the Supporting Information).[43] In our previous studies, these event types were demonstrated to enter the nanopore with different frequencies based on their shape; therefore, correction factors for this event frequency bias were applied to the current data, in which the hybrid 1, hybrid 2, and triplexlike intermediate had relative event frequencies of 1.1, 1.0, and 6.2, respectively.[43] To briefly reiterate, the major event types observed were characteristic of the hybrid folds [∼75% (Figure S3 of the Supporting Information)]. These events gave different current signatures that oscillated between a deep current level ($I$) and a midcurrent level [$I_M$ (Figure 3a)]. Furthermore, the midcurrent levels were distinct and assigned as hybrid 1 ($I_M/I_0$ = 37 ± 3%) and hybrid 2 ($I_M/I_0$ = 44 ± 4%) on the basis of our previous work.[43] Hybrid 1 was shown to be more abundant than hybrid 2 with a ratio of approximately 2:1. The statistical analysis of the event types corresponding to hybrid 1 and hybrid 2 is presented in Figure 3b. Second, current signatures for the loop entry were analyzed and corresponded to ∼20% of the event types, while event types for the triplexlike fold represented ∼5% of the population. Only the triplexlike folded structures were able to unravel and translocate the narrow $\beta$-barrel of the ion channel; the hybrid G-quadruplexes were too stable inside the nanocavity of $\alpha$-HL to unfold on the millisecond time frame of the analysis, and they eventually exited from the *cis* side of the protein vestibule by diffusional motion.

The G-quadruplexes that contained UV-induced damage in the 3′ loop, middle loop, or the 5′ loop presented three types of ion−current events that were similar to that of the native sequence. The hybrid event types were slightly less frequent [60−70% (Figure S3 of the Supporting Information)] than that observed for the undamaged G-quadruplex. Hybrid 1 and 2 distributions for the ODNs containing the T=T at the 3′ loop and the middle loop gave a similar 2:1 ratio, as observed in the native sequence. This observation is interpreted to say that incorporation of T=T into the 3′ or middle loops of a hybrid quadruplex does not alter the hybrid structural distribution. The presence of the T=T in the 5′ loop of the G-quadruplex caused a shift in the hybrid 1 and 2 equilibrium that favored hybrid 2 (Figure 3b). We hypothesize that the presence of T=T in the double-chain reversal loop caused the equilibrium between the hybrids to change in favor of hybrid 2, in which the damage was placed in the edgewise loop. This hypothesis was further explored by examining the basket fold that does not have a double-chain reversal, and the propeller fold that has only double-chain reversal loops.

The remainder of the event types observed in the T=T-containing quadruplexes were characteristic of the loop entry and the triplexlike folding intermediate. The frequency of loop entry in all damaged quadruplexes was similar to that observed in the native sequence [∼20% (Figure S3 of the Supporting Information)]. Finally, the observed percentage of triplexlike events was slightly higher than that of the natural sequence [∼5% (Figure S3 of the Supporting Information)]. This observation was expected on the basis of the lower $T_m$ values for the damage-containing strands. Another possible structure for the human telomere sequence in KCl solution was characterized as a basket fold with two tetrads that results when the 5′ TA tail is removed and the 3′ tail is truncated to a single T.[51] In the study presented here, the natural form of the human telomere sequence was studied with 5′ TA and 3′ TT tails that was shown by nuclear magnetic resonance (NMR) to adopt the hybrid folds;[12,13] therefore, a two-tetrad basket fold was not expected in these studies. In summary, the $\alpha$-HL experiment allowed us to determine that T=Ts in the loops of G-quadruplexes show a favorability for edgewise loops over double-chain reversal loops that could not have been determined by CD, EMSA, or $T_m$ experiments.

**Basket Fold.** In NaCl solutions, the human telomere sequence assumes a basket fold that consists of two edgewise loops and one diagonal loop (Figure 4a). The basket fold can interact with the $\alpha$-HL in two different manners. (1) It enters the vestibule, unravels, threads into the narrow constriction zone of the $\beta$-barrel with either of the two-nucleotide overhang tails, and translocates across the pore, or (2) it enters the vestibule from the loop side with both overhangs distant from the constriction; thus, it is unable to thread and translocate until the molecule escapes back to the *cis* side of the protein channel in a diffusion-controlled process.[44,52] Similar to the case for the native sequence, the damage-containing ODNs folded in a basket fashion featured the same event distributions: one that translocated across the $\alpha$-HL channel presenting a deep current blockage (pattern 1, Figure 4b) and one that did not translocate through the channel presenting a shallower current blockage (pattern 2, Figure 4b). Moreover, the deep current blockage event type was modestly sensitive to increased voltage, giving an inverse correlation, indicating that it unravels and translocates to the *trans* side of the pore (Figure 4c). The


dx.doi.org/10.1021/bi501072m | *Biochemistry* 2014, 53, 7484−7493

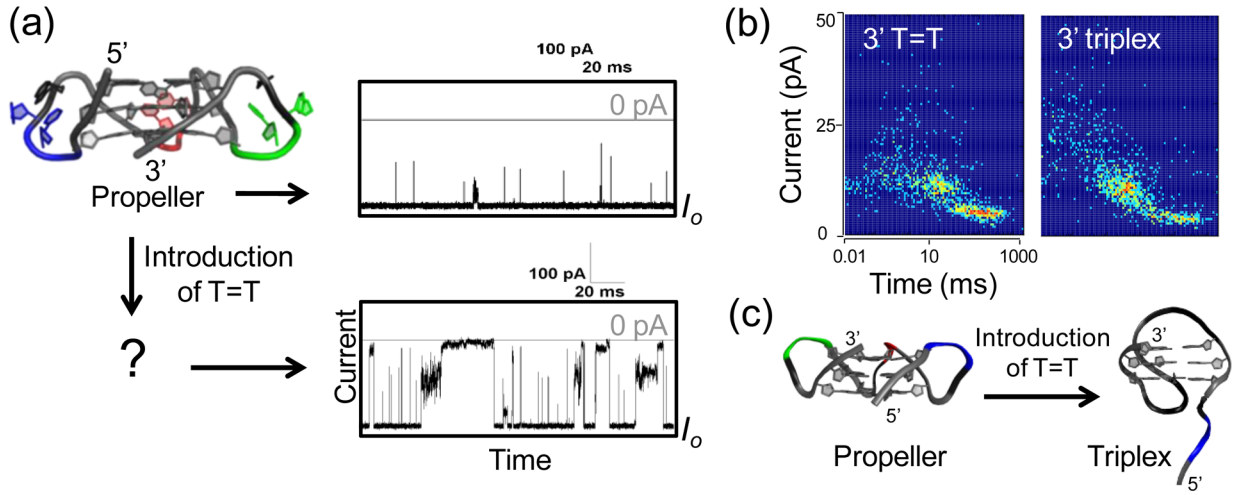


**Figure 5.** Nanopore analysis of the T=T-containing human telomere sequence in 5 M LiCl. (a) Undamaged propeller fold (PDB entry 1KF1)[16] structure and typical nanopore experiment $i-t$ traces. The intact propeller fold oligomer is too large to enter the vestibule of the $\alpha$-HL; therefore, there are no translocation events. Once the damage is introduced, long, deep blockage events that might correspond to a triplexlike structure caused by the partial unfolding of the propeller due to the damage are observed. (b) Representative heat plot of the T=T-containing telomere sequence and a triplex-forming sequence where Gs have been substituted with Ts at either the 5′ or 3′ ends. (c) Proposed structure based on ref 49.

shallow current blockage gave a time distribution with change in the voltage that was shallow and was interpreted to indicate a diffusion-controlled process back out the *cis* opening of the pore. These results are interpreted to mean that the T=T in a basket fold does not affect the structure of the G-quadruplex significantly. Further, this single-molecule experiment supports the conclusions drawn from the $T_m$ and CD experiments in which incorporation of a T=T in an edgewise or diagonal loop is not very destabilizing to the secondary structure.

**Propeller Fold.** Under dehydrating conditions (5 M LiCl), the human telomere sequence can assume the propeller fold (all double-chain reversal loops) in the presence of $K^+$.[17,18,53] The intact propeller fold was too large [~4 nm (Figure 1)] to enter the vestibule of the $\alpha$-HL nanopore [~3.0 nm (Figure 1)]; therefore, the only events detected during the nanopore study were very short spikes caused by random interactions of the G-quadruplex with the mouth of the vestibule (Figure 5a). This observation was previously reported by our laboratory.[44] When a T=T was introduced into the sequence, deep current blockage events were recorded as shown in the bottom $i-t$ trace in Figure 5a. Two distinct current versus time populations were observed in heat plots of the data (Figure 5b and Figure S6 of the Supporting Information). We interpret these two populations to represent different entry orientations of the ODN. On the basis of our previous knowledge from the hybrid studies, T=T is not preferred in a double-chain reversal loop. Therefore, the T=T can unwind the propeller fold to a triplexlike structure that has a head with a loop and a tail comprised of eight nucleotides (Figure 5c). Correlating with the $T_m$ data, the shortest translocation time was observed for the ODN that contained the T=T in the middle of the structure (Table 2 and Figure S5 of the Supporting Information). The T=T in the middle loop would have the largest effect on the ability of the ODN to fold, explaining its lower $T_m$ value and the shorter translocation time (Figure S5 of the Supporting Information).

Two lines of evidence support the hypothesis that incorporation of T=T into a propeller G-quadruplex yields a triplexlike structure. First, the CD spectra for the T=T-containing quadruplexes in 5 M LiCl give similar spectra ($\lambda_{max}$ = 264 nm, and $\lambda_{min}$ = 240 nm) as reported by Sugiyama and coworkers for the triplex-forming sequence.[49] Second, a series of control strands was designed to model the triplex species induced by the T=T, in which the terminal 5′ or 3′ GGG was converted to a 5′ or 3′ TTT, respectively. These control sequences had an eight-nucleotide tail on the 5′ or 3′ end. Nanopore analysis of these control strands also gave two current−time populations in the heat plots shown in Figure 5b. These control studies yielded data that were similar to the data collected for T=T-containing quadruplexes, which are interpreted to mean that T=T causes the double-chain reversal loop to unwind giving a structure that behaves like the nanopore as a control strand that can adopt a triplexlike structure. Recent molecular dynamic simulations identified that the parallel triplex is not stable compared to the antiparallel triplex;[54] because CD data dos not exist for the parallel triplex, we cannot determine the exact strand orientation for these strands in our studies. Additionally, the current data point toward the triplex fold as the structure formed when T=T is present in the propeller fold; however, until the triplex is adequately characterized by NMR or X-ray methods, it will remain elusive, but this structure provides the best explanation for a number of previous experimental observations and the results presented here.[18,43,49,50] This observation further supports our hypothesis that T=Ts inhibit double-chain reversal loop formation.

## DISCUSSION

In this work, established methods were used to study how UV-induced damage affects the structure of the human telomere G-quadruplex folds. Utilizing CD and EMSA techniques, it was found that the hybrid and basket folds are formed regardless of the loop in which the T=T was placed (Figure 2 and Figure S2 of the Supporting Information). The $T_m$ results suggest that T=Ts cause a moderate decrease (~5 °C) in the thermal stability of hybrid and basket folds (Table 2). Similar to the current results, the introduction of thymine glycol[36] or 8-oxo-A[38] into a loop was not detrimental to the hybrid or basket structure based on CD and EMSA experiments. Furthermore, introduction of T=T or thymine glycol into a loop of a G-quadruplex induced only a moderate decrease in the thermal


dx.doi.org/10.1021/bi501072m | *Biochemistry* 2014, 53, 7484−7493

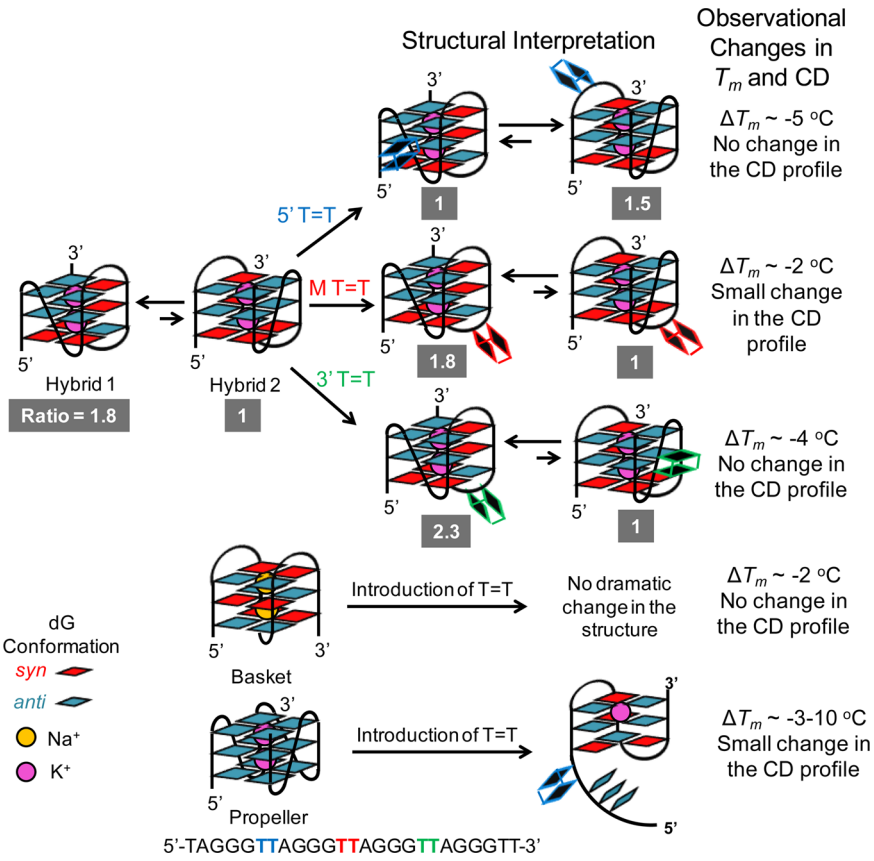


**Figure 6.** Summary of the structural interpretation of the nanopore data and observational changes in the $T_m$ and CD measurements.

stability. Contrary to these results, the introduction of 8-oxo-A into the loops caused a significant increase in the $T_m$.[38] These data are interpreted to mean that the cyclobutane ring of the T=T restricts the conformational flexibility of the loops that leads to a subtle decrease in stability without altering the overall fold for hybrid and basket G-quadruplexes. In contrast to these observations, T=T in the human telomere sequence under propeller folding conditions demonstrated the largest effect on the thermal stabilities (Table 2). In addition, the CD spectrum showed that the fold resembles a triplexlike structure and not a propeller fold.[48,49] The conventional studies performed yielded interesting results. However, they were inadequate to predict the changes that introduction of the T=T causes to the G-quadruplex fold. Therefore, we utilized a single-molecule method that was recently shown to be an excellent tool for observing the different folds of the G-quadruplex.[43] The nanopore measurements gave us a unique opportunity to further explore how UV-induced DNA damage affects folding of the human telomeric G-quadruplexes under different physical conditions.

The $\alpha$-HL nanopore has been extensively used to study nucleic acids.[55−57] A simple G-quadruplex containing only two tetrads [thrombin binding aptamer (TBA)] was first studied using $\alpha$-HL regarding its cation affinities, followed by the studies of thrombin−TBA interactions.[58−62] Later, the human telomere sequence and the different folds that G-quadruplex can assume were studied by our laboratory.[43,44] The ability of $\alpha$-HL to distinguish between different G-quadruplex folds is attributed, among others, to the recently discovered sensing zone that is located in the vestibule rather than in the $\beta$-barrel of the protein ion channel.[44,63] The vestibule of the $\alpha$-HL (~3.0 nm) was shown to exclude the propeller fold (1.8 nm × 4.0 nm), because its dimensions are too large for it to enter (Figure 1).[44] The hybrid folds were barely able to enter (2.7 nm × 3.0 nm), and therefore, even the slight difference in shape between hybrid 1 and hybrid 2 gave different signals.[43] Finally, the basket fold (2.4 nm × 2.8 nm) was small enough to easily enter and translocate across the pore.[44] In this study, we have shown using the nanopore method that when the T=T was introduced into a double-chain reversal loop of the hybrid fold the equilibrium between the hybrids changed to favor the conformation with T=T positioned in an edgewise loop (Figure 6). This hypothesis was further supported by examining the other folds of the human telomere sequence: propeller (all double-chain reversal loops) and basket (no double-chain reversal loops). The T=T-containing basket fold showed the same type of events as the natural sequence, whereas propeller folding conditions showed events that were similar to those of a triplexlike fold, thus supporting our hypothesis that T=Ts are not well accommodated in the double-chain reversal loop (Figure 6). These results are interpreted to mean that locking the loop Ts by cyclobutane dimerization causes the loop topology to be hindered in a way that does not favor double-chain reversal loop formation.

The hybrid fold is the proposed topology of the G-quadruplex that the telomere region assumes *in vivo*.[13,21,23] Hybrids can adopt two different folds positioning the double-chain reversal loop at the 3′ or 5′ terminus of the G-quadruplex (Figure 6). The ability of the hybrid to change from hybrid 1 to hybrid 2 allows the fold to accommodate the T=T damage without significant structural perturbations. This quality of the telomere is crucial for its function because the region is


dx.doi.org/10.1021/bi501072m | *Biochemistry* 2014, 53, 7484−7493

hypersensitive to UV-induced damage.[27] Telomere damage that causes a change in the folding pattern (e.g., G oxidation products)[35] is proposed to induce telomere shortening that ultimately leads to cell death.[30] The single-stranded portion of the telomere is protected from degradation and RPA recognition by the overhang binding protein POT1 and TTP1.[25,64] It was recently shown by Ray et al.[24] that the hybrid fold is crucial for POT1 binding. Therefore, DNA damage that significantly affects the G-quadruplex structure will decrease the extent of binding of the POT1−TTP1 complex *in vivo*, in a fashion analogous to that of G oxidation products that significantly impact the structural fold.[29] However, on the basis of the results presented here, T=T does not greatly affect the overall topology of the G-quadruplex hybrid fold; therefore, photodamaged telomeric sequences do not lose protection by POT1−TTP1 complex binding and, ultimately, do not cause telomere shortening in contrast to damage from G oxidation. These data demonstrate that T=Ts are accommodated in the G-quadruplex folds of the human telomere sequence, and therefore, damage can accumulate without causing significant structural perturbations leading to telomere truncation. On the other hand, G-quadruplex-forming sequences that favor an all-parallel propeller fold are now predicted to be markedly destabilized if thymine photodimers are formed in their loop regions (Figure 6).

## CONCLUSIONS

Following the traditional procedures for analyzing G-quadruplexes (CD, $T_m$, and EMSA), we demonstrated that the presence of T=T damage does not significantly distort the overall secondary structure and only slightly decreases the stabilities of hybrid and basket folds (Figure 2, Figure S2 of the Supporting Information, and Table 2). To gain more insight into the structural changes that can arise from T=T formation in telomeres, we used the $\alpha$-HL nanopore to capture and analyze the damaged folds at a single-molecule level. From these experiments, we established that the presence of a T=T in the hybrid folds changed the ratio of the hybrid types to favor the conformation that positions the damaged site at an edgewise loop instead of a double-chain reversal loop. This observation was further verified by examining the basket fold (edgewise and diagonal loops) and the propeller fold (all double-chain reversal loops), in which the basket fold was not altered by T=Ts and the structure for the propeller topology was significantly impacted.

In cells, the predominant G-quadruplex structure for the natural human telomere sequence is proposed to be the hybrid fold, based on the $K^+$ concentration inside the cell and its binding affinity for the G-quadruplex.[13,21,23] Once the T=T is present, the shape of the structure remains predominantly the same, aside from the hybrid 1 to hybrid 2 ratio when the damage is located in the double-chain reversal loop. This observation explains why the telomere can still maintain its functions and does not undergo shortening even after extensive UV irradiation.[27] Even if the T=T is present in the hybrid fold, the damage does not affect the overall shape of the fold, making it possible for the POT1 and TPP1 proteins to bind and maintain proper function. Therefore, hybrid G-quadruplexes can mask any detrimental structural consequences of T=Ts in the cell.

## ASSOCIATED CONTENT

### Supporting Information

Representative traces for $T_m$, HPLC, and ion current recordings. This material is available free of charge via the Internet at http://pubs.acs.org.

## AUTHOR INFORMATION

### Corresponding Author

*E-mail: burrows@chem.utah.edu. Phone: (801) 585-7290. Fax: (801) 585-0024.

### Funding

We are grateful for National Institutes of Health Grant R01 GM093099 and National Science Foundation Grant CHE-1152533.

### Notes

The authors declare no competing financial interest.

## ACKNOWLEDGMENTS

We appreciate thoughtful conversations with Prof. Henry S. White, Dr. Na An, and Yun Ding (University of Utah) and Dr. Geoffrey Barrall at Electronic BioSciences, and we appreciate the donation of the EBS ion channel recording instrumentation used in the experiments described herein.

## REFERENCES

(1) Roderick, J. O. S., and Jan, K. (2010) Telomeres: Protecting chromosomes against genome instability. *Nat. Rev. Mol. Cell Biol. 11*, 171−181.

(2) Osterhage, J. L., and Friedman, K. L. (2009) Chromosome end maintenance by telomerase. *J. Biol. Chem. 284*, 16061−16065.

(3) Moyzis, R. K., Buckingham, J. M., Cram, L. S., Dani, M., Deaven, L. L., Jones, M. D., Meyne, J., Ratliff, R. L., and Wu, J. R. (1988) A highly conserved repetitive DNA sequence, $(TTAGGG)_n$, present at the telomeres of human chromosomes. *Proc. Natl. Acad. Sci. U.S.A. 85*, 6622−6626.

(4) Biffi, G., Tannahill, D., McCafferty, J., and Balasubramanian, S. (2013) Quantitative visualization of DNA G-quadruplex structures in human cells. *Nat. Chem. 5*, 182−183.

(5) Sen, D., and Gilbert, W. (1988) Formation of parallel four-stranded complexes by guanine-rich motifs in DNA and its implications for meiosis. *Nature 334*, 364−366.

(6) Cahoon, L. A., and Seifert, H. S. (2009) An alternative DNA structure is necessary for pilin antigenic variation in *Neisseria gonorrhoeae*. *Science 325*, 764−767.

(7) Rodriguez, R., Miller, K. M., Forment, J. V., Bradshaw, C. R., Nikan, M., Britton, S., Oelschlaegel, T., Xhemalce, B., Balasubramanian, S., and Jackson, S. P. (2012) Small-molecule-induced DNA damage identifies alternative DNA structures in human genes. *Nat. Chem. Biol. 8*, 301−310.

(8) Cheung, I., Schertzer, M., Rose, A., and Lansdorp, P. M. (2002) Disruption of dog-1 in *Caenorhabditis elegans* triggers deletions upstream of guanine-rich DNA. *Nat. Genet. 31*, 405−409.

(9) Siddiqui-Jain, A., Grand, C. L., Bearss, D. J., and Hurley, L. H. (2002) Direct evidence for a G-quadruplex in a promoter region and its targeting with a small molecule to repress c-MYC transcription. *Proc. Natl. Acad. Sci. U.S.A. 99*, 11593−11598.

(10) Osterhage, J. L., and Friedman, K. L. (2009) Chromosome end maintenance by telomerase. *J. Biol. Chem. 284*, 16061−16065.

(11) Xu, Y. (2011) Chemistry in human telomere biology: Structure, function and targeting of telomere DNA/RNA. *Chem. Soc. Rev. 40*, 2719−2740.

(12) Phan, A. T., Kuryavyi, V., Luu, K. N., and Patel, D. J. (2007) Structure of two intramolecular G-quadruplexes formed by natural human telomere sequences in $K^+$ solution. *Nucleic Acids Res. 35*, 6517−6525.

(13) Ambrus, A., Chen, D., Dai, J., Bialis, T., Jones, R. A., and Yang, D. (2006) Human telomeric sequence forms a hybrid-type intramolecular G-quadruplex structure with mixed parallel/antiparallel strands in potassium solution. *Nucleic Acids Res. 34*, 2723−2735.
(14) Xu, Y., Noguchi, Y., and Sugiyama, H. (2006) The new models of the human telomere d[AGGG(TTAGGG)$_3$] in K$^+$ solution. *Bioorg. Med. Chem. 14*, 5584−5591.
(15) Wang, Y., and Patel, D. J. (1993) Solution structure of the human telomeric repeat d[AG$_3$(T$_2$AG$_3$)$_3$] G-tetraplex. *Structure 1*, 263−282.
(16) Parkinson, G. N., Lee, M. P. H., and Neidle, S. (2002) Crystal structure of parallel quadruplexes from human telomeric DNA. *Nature 417*, 876−880.
(17) Heddi, B., and Phan, A. T. (2011) Structure of human telomeric DNA in crowded solution. *J. Am. Chem. Soc. 133*, 9824−9833.
(18) Gray, R. D., Buscaglia, R., and Chaires, J. B. (2012) Populated intermediates in the thermal unfolding of the human telomeric quadruplex. *J. Am. Chem. Soc. 134*, 16834−16844.
(19) Miller, M. C., Buscaglia, R., Chaires, J. B., Lane, A. N., and Trent, J. O. (2010) Hydration is a major determinant of the G-quadruplex stability and conformation of the human telomere 3′ sequence of d(AG$_3$(TTAG$_3$)$_3$. *J. Am. Chem. Soc. 132*, 17105−17107.
(20) Patel, D. J., Phan, A. T., and Kuryavyi, V. (2007) Human telomere, oncogenic promoter and 5′-UTR G-quadruplexes: Diverse higher order DNA and RNA targets for cancer therapeutics. *Nucleic Acids Res. 35*, 7429−7455.
(21) Yang, D., and Okamoto, K. (2010) Structural insights into G-quadruplexes: Towards new anticancer drugs. *Future Med. Chem. 2*, 619−646.
(22) Lane, A. N., Chaires, J. B., Gray, R. D., and Trent, J. O. (2008) Stability and kinetics of G-quadruplex structures. *Nucleic Acids Res. 36*, 5482−5515.
(23) Hänsel, R., Löhr, F., Foldynová-Trantírková, S., Bamberg, E., Trantírek, L., and Dötsch, V. (2011) The parallel G-quadruplex structure of vertebrate telomeric repeat sequences is not the preferred folding topology under physiological conditions. *Nucleic Acids Res. 39*, 5768−5775.
(24) Ray, S., Bandaria, J. N., Qureshi, M. H., Yildiz, A., and Balci, H. (2014) G-quadruplex formation in telomeres enhances POT1/TPP1 protection against RPA binding. *Proc. Natl. Acad. Sci. U.S.A. 111*, 2990−2995.
(25) He, Q., Zeng, P., Tan, J.-H., Ou, T.-M., Gu, L.-Q., Huang, Z.-S., and Li, D. (2014) G-quadruplex-mediated regulation of telomere binding protein POT1 gene expression. *Biochim. Biophys. Acta 1840*, 2222−2233.
(26) Song, L., Hobaugh, M. R., Shustak, C., Cheley, S., Bayley, H., and Gouaux, J. E. (1996) Structure of *Staphylococcal* α-hemolysin, a heptameric transmembrane pore. *Science 274*, 1859−1865.
(27) Rochette, P. J., and Brash, D. E. (2010) Human telomeres are hypersensitive to UV-induced DNA damage and refractory to repair. *PLoS Genet. 6*, e1000926.
(28) Henle, E. S., Han, Z., Tang, N., Rai, P., Luo, Y., and Linn, S. (1999) Sequence-specific DNA cleavage by Fe$^{2+}$-mediated Fenton reactions has possible biological implications. *J. Biol. Chem. 274*, 962−971.
(29) Oikawa, S., Tada-Oikawa, S., and Kawanishi, S. (2001) Site-specific DNA damage at the GGG sequence by UVA involves acceleration of telomere shortening. *Biochemistry 40*, 4763−4768.
(30) Verdun, R. E., and Karlseder, J. (2007) Replication and protection of telomeres. *Nature 447*, 924−931.
(31) Samassekou, O., Gadji, M., Drouin, R., and Yan, J. (2010) Sizing the ends: Normal length of human telomeres. *Ann. Anat. 192*, 284−291.
(32) Wolkowitz, O. M., Mellon, S. H., Epel, E. S., Lin, J., Dhabhar, F. S., Su, Y., Reus, V. I., Rosser, R., Burke, H. M., Kupferman, E., Compagnone, M., Nelson, J. C., and Blackburn, E. H. (2011) Leukocyte telomere length in major depression: Correlations with chronicity, inflammation and oxidative stress—preliminary findings. *PLoS One 6*, e17837.
(33) Steenken, S., and Jovanovic, S. (1997) How easily oxidizable is DNA? One-electron reduction potentials of adenosine and guanosine radicals in aqueous solution. *J. Am. Chem. Soc. 119*, 617−618.
(34) Burrows, C. J., and Muller, J. G. (1998) Oxidative nucleobase modifications leading to strand scission. *Chem. Rev. 98*, 1109−1152.
(35) Fleming, A. M., and Burrows, C. J. (2013) G-quadruplex folds of the human telomere sequence alter the site reactivity and reaction pathway of guanine oxidation compared to duplex DNA. *Chem. Res. Toxicol. 26*, 593−607.
(36) Zhou, J., Liu, M., Fleming, A. M., Burrows, C. J., and Wallace, S. S. (2013) Neil3 and NEIL1 DNA glycosylases remove oxidative damages from quadruplex DNA and exhibit preferences for lesions in the telomeric sequence context. *J. Biol. Chem. 288*, 27263−27272.
(37) Fleming, A. M., Orendt, A. M., He, Y., Zhu, J., Dukor, R. K., and Burrows, C. J. (2013) Reconciliation of chemical, enzymatic, spectroscopic and computational data to assign the absolute configuration of the DNA base lesion spiroiminodihydantoin. *J. Am. Chem. Soc. 135*, 18191−18204.
(38) Aggrawal, M., Joo, H., Liu, W., Tsai, J., and Xue, L. (2012) 8-Oxo-7,8-dihydrodeoxyadenosine: The first example of a native DNA lesion that stabilizes human telomeric G-quadruplex DNA. *Biochem. Biophys. Res. Commun. 421*, 671−677.
(39) Sinha, R. P., and Hader, D. P. (2002) UV-induced DNA damage and repair: A review. *Photochem. Photobiol. Sci. 1*, 225−236.
(40) Norval, M., Lucas, R. M., Cullen, A. P., de Gruijl, F. R., Longstreth, J., Takizawa, Y., and van der Leun, J. C. (2011) The human health effects of ozone depletion and interactions with climate change. *Photochem. Photobiol. Sci. 10*, 199−225.
(41) Su, D. G. T., Fang, H., Gross, M. L., and Taylor, J.-S. A. (2009) Photocrosslinking of human telomeric G-quadruplex loops by anti cyclobutane thymine dimer formation. *Proc. Natl. Acad. Sci. U.S.A. 106*, 12861−12866.
(42) Smith, J. E., Lu, C., and Taylor, J.-S. (2014) Effect of sequence and metal ions on UVB-induced anti cyclobutane pyrimidine dimer formation in human telomeric DNA sequences. *Nucleic Acids Res. 42*, 5007−5019.
(43) An, N., Fleming, A. M., and Burrows, C. J. (2013) Interactions of the human telomere sequence with the nanocavity of the α-hemolysin ion channel reveal structure-dependent electrical signatures for hybrid folds. *J. Am. Chem. Soc. 135*, 8562−8570.
(44) An, N., Fleming, A. M., Middleton, E. G., and Burrows, C. J. (2014) Size-selective property of α-hemolysin provides signatures for DNA nanostructures formed by the human telomere sequence. *Proc. Natl. Acad. Sci. U.S.A. 111*, 14325−14331.
(45) Nguyen, K. V., and Burrows, C. J. (2011) A prebiotic role for 8-oxoguanosine as a flavin mimic in pyrimidine dimer photorepair. *J. Am. Chem. Soc. 133*, 14586−14589.
(46) Zhang, B., Galusha, J., Shiozawa, P. G., Wang, G., Bergren, A. J., Jones, R. M., White, R. J., Ervin, E. N., Cauley, C. C., and White, H. S. (2007) Bench-top method for fabricating glass-sealed nanodisk electrodes, glass nanopore electrodes, and glass nanopore membranes of controlled size. *Anal. Chem. 79*, 4778−4787.
(47) White, R. J., Ervin, E. N., Yang, T., Chen, X., Daniel, S., Cremer, P. S., and White, H. S. (2007) Single ion-channel recordings using glass nanopore membranes. *J. Am. Chem. Soc. 129*, 11766−11775.
(48) Karsisiotis, A. I., Hessari, N. M. A., Novellino, E., Spada, G. P., Randazzo, A., and Webba da Silva, M. (2011) Topological characterization of nucleic acid G-quadruplexes by UV absorption and circular dichroism. *Angew. Chem., Int. Ed. 50*, 10645−10648.
(49) Koirala, D., Mashimo, T., Sannohe, Y., Yu, Z., Mao, H., and Sugiyama, H. (2012) Intramolecular folding in three tandem guanine repeats of human telomeric DNA. *Chem. Commun. 48*, 2006−2008.
(50) Rajendran, A., Endo, M., Hidaka, K., and Sugiyama, H. (2014) Direct and single-molecule visualization of the solution-state structures of G-hairpin and G-triplex intermediates. *Angew. Chem., Int. Ed. 53*, 4107−4112.
(51) Lim, K. W., Amrane, S., Bouaziz, S., Xu, W., Mu, Y., Patel, D. J., Luu, K. N., and Phan, A. T. (2009) Structure of the human telomere in

$K^+$ solution: A stable basket-type G-quadruplex with only two G-tetrad layers. *J. Am. Chem. Soc. 131*, 4301−4309.
(52) Vercoutere, W. A., Winters-Hilt, S., DeGuzman, V. S., Deamer, D., Ridino, S. E., Rodgers, J. T., Olsen, H. E., Marziali, A., and Akeson, M. (2003) Discrimination among individual Watson-Crick base pairs at the termini of single DNA hairpin molecules. *Nucleic Acids Res. 31*, 1311−1318.
(53) Lannan, F. M., Mamajanov, I., and Hud, N. V. (2012) Human telomere sequence DNA in water-free and high-viscosity solvents: G-quadruplex folding governed by Kramers rate theory. *J. Am. Chem. Soc. 134*, 15324−15330.
(54) Stadlbauer, P., Trantirek, L., Cheatham, T. E., III, Koca, J., and Sponer, J. (2014) Triplex intermediates in folding of human telomeric quadruplexes probed by microsecond-scale molecular dynamics simulations. *Biochimie 105*, 22−35.
(55) Branton, D., Deamer, D. W., Marziali, A., Bayley, H., Benner, S. A., Butler, T., Di Ventra, M., Garaj, S., Hibbs, A., Huang, X., Jovanovich, S. B., Krstic, P. S., Lindsay, S., Ling, X. S., Mastrangelo, C. H., Meller, A., Oliver, J. S., Pershin, Y. V., Ramsey, J. M., Riehn, R., Soni, G. V., Tabard-Cossa, V., Wanunu, M., Wiggin, M., and Schloss, J. A. (2008) The potential and challenges of nanopore sequencing. *Nat. Biotechnol. 26*, 1146−1158.
(56) Cherf, G. M., Lieberman, K. R., Rashid, H., Lam, C. E., Karplus, K., and Akeson, M. (2012) Automated forward and reverse ratcheting of DNA in a nanopore at 5-Å precision. *Nat. Biotechnol. 30*, 344−348.
(57) Kasianowicz, J. J., Brandin, E., Branton, D., and Deamer, D. W. (1996) Characterization of individual polynucleotide molecules using a membrane channel. *Proc. Natl. Acad. Sci. U.S.A. 93*, 13770−13773.
(58) Shim, J., and Gu, L.-Q. (2012) Single-molecule investigation of G-quadruplex using a nanopore sensor. *Methods 57*, 40−46.
(59) Shim, J. W., Tan, Q., and Gu, L.-Q. (2009) Single-molecule detection of folding and unfolding of the G-quadruplex aptamer in a nanopore nanocavity. *Nucleic Acids Res. 37*, 972−982.
(60) Rotem, D., Jayasinghe, L., Salichou, M., and Bayley, H. (2012) Protein detection by nanopores equipped with aptamers. *J. Am. Chem. Soc. 134*, 2781−2787.
(61) Renner, S., Geltinger, S., and Simmel, F. C. (2010) Nanopore translocation and force spectroscopy experiments in microemulsion droplets. *Small 6*, 190−194.
(62) Gu, L.-Q., and Shim, J. W. (2010) Single molecule sensing by nanopores and nanopore devices. *Analyst 135*, 441−451.
(63) Jin, Q., Fleming, A. M., Johnson, R. P., Ding, Y., Burrows, C. J., and White, H. S. (2013) Base-excision repair activity of uracil-DNA glycosylase monitored using the latch zone of $\alpha$-hemolysin. *J. Am. Chem. Soc. 135*, 19347−19353.
(64) Blasco, M. A. (2007) Telomere length, stem cells and aging. *Nat. Chem. Biol. 3*, 640−649.